

# Mechanism of Dangling Bond Elimination on As-rich InGaAs Surface

Wilhelm Melitz<sup>1,2</sup>, Evgeni Chagarov<sup>2</sup>, Tyler Kent<sup>1,2</sup>, Ravi Droopad<sup>3</sup>, Jaesoo Ahn<sup>4</sup>, Rathnait Long<sup>4</sup>, Paul C. McIntyre<sup>4</sup> and Andrew C. Kummel<sup>2\*</sup> [akummel@ucsd.edu](mailto:akummel@ucsd.edu)

<sup>1</sup>Mat. Sci. & Eng., <sup>2</sup>Dept. of Chem/Biochem, Univ. Cal., San Diego, La Jolla, CA, 92093 USA

<sup>3</sup>Dept. Physics, Texas State U., San Marcos, TX 78666 USA

<sup>4</sup>Dept Mat. Sci. Eng., Stanford U., Stanford, CA, 94305 USA

## Abstract

This work demonstrates with STM, STS, DFT, and device studies that TMA prepulsing on the As-rich InGaAs (2x4) surface reduces the trap state density by reducing As-As dimer bonds and As dangling bonds.

## Introduction

A MOSCAP study by Huang *et al.* has shown that trimethylaluminum (TMA) based a-Al<sub>2</sub>O<sub>3</sub> (a = amorphous) oxide growth at single elevated temperature on As-rich InGaAs(001)-(2×4) produces a lower D<sub>it</sub> in comparison to the TMA dosing at elevated temperature on In/Ga-rich (4×2) [1]. Although the (2×4) surface may be more prone to formation of As oxides during ALD oxide growth, TMA is known to bond strongly to As atoms and therefore to be more efficient for reducing As<sub>2</sub>O<sub>3</sub> formation than reducing Ga or In oxide formation [2; 3]. Scanning tunneling microscopy (STM) and density functional theory (DFT) demonstrates the thermodynamically favorable bonding of TMA on the InGaAs(001)-(2×4) surface to As-dimers. DFT modeling shows that the bonding of TMA to the As-dimers restores the As to tetrahedral bonding, eliminating the dangling bonds and thereby generating an electrically passivated surface with low midgap states. For the As-rich (2×4) reconstruction, the bonding of the TMA reaction products and the passivation of the dangling bonds is consistent with the chemical driving force being the formation of As-Al-As bonds that would generate a high nucleation density of adsorbed dimethylaluminums (DMA).

## Experimental

In the present STM/STS study, As “capped” samples are employed to avoid oxidation and contamination of the InGaAs surface prior to TMA dosing. Further details concerning the decapped samples and preparation methods are published in references [4; 5]. The deposition of TMA is performed in the load lock, allowing for sample transfer *in situ*, to both the preparation chamber for PDA and the STM/STS chamber for analysis without contamination.

## Scanning Probe Microscopy Studies

The filled state STM image of the degassed, decapped, clean In<sub>0.53</sub>Ga<sub>0.47</sub>As(001)-(2×4) surface reconstruction can be seen in Fig. 1(a). The characteristic zig-zag shape of the rows are due to the presence of a mixture of wide double As dimer unit cells denoted as β2(2×4) and narrow single dimer unit cells denoted as α2(2×4) as shown in Fig. 1(b). Models of the double and single dimer unit cells are shown in Fig. 1(c) and 1(d).

Fig. 2(a) is a STM image of a 5L dose of TMA at 280 °C on a decapped As-rich In<sub>0.53</sub>Ga<sub>0.47</sub>As (001)-(2×4) surface. The blue square indicates a bright feature, consistent with a dangling bond. These dangling bonds are most likely unreacted sites or As adatoms. At high doses, these bright features are nearly eliminated showing that TMA can passivate the dangling bonds. Single point spectroscopy of the bright and dark features (Fig. 2) is consistent with presence of dangling bonds on the bright sites. The STS signal is proportional to the local density of states (LDOS) and the zero sample bias is the Fermi level position of the surface relative to the bands. The STS was performed with a modulation frequency of 1 kHz, a lock-in time constant of 20 ms, and a T-raster of 40 ms; therefore, it is sensitive to all trap states with a lifetime less than 1 ms. The blue solid spectra (minority bright sites) shows a large peak in the LDOS near the conduction band (CB) edge, while the green solid curve (majority adsorbate covered sites) does not have a conduction band edge DOS peak. For all TMA dosed surfaces including full coverage, the surface Fermi level is closer to the CB on an n-type sample, consistent with the surface being partially unpinned.

## Density Functional Theory Simulations

In order to determine the surface bonding configuration of TMA on the As-rich In<sub>0.53</sub>Ga<sub>0.47</sub>As (001)-(2×4), DFT was employed to model multiple bonding geometries on In<sub>0.5</sub>Ga<sub>0.5</sub>As(001)-(2×4) since the STM data does not have sufficient resolution to give the exact atomic structure. All DFT simulations were performed with the Vienna Ab-Initio Simulation Package (VASP) [6; 7] using projector augmented-wave (PAW) pseudopotentials (PP) [8] [9] and the PBE (Perdew-Burke-Ernzerhof) exchange-correlation functional [10; 11]. The choice of PBE functional and PAW PP was validated by parameterization runs demonstrating good reproducibility of experimental lattice constants, bulk moduli, and formation/cohesive energies for bulk crystalline InGaAs and its components: GaAs and InAs.

Fig. 3(a) shows a unit cell containing two rows of As-dimers. The bonding sites and energies were determined via DFT calculations using DMA and monomethylaluminum (MMA) [12] for three and six adsorbates, consistent with half and full coverage. The DMA DFT model for the half and full coverage on the (2×4) unit cell containing two row As-dimers is shown in Fig. 3(b) and 3(c). While the half coverage DMA has As atoms with highly strained bonds, for full coverage DMA, all the As atoms have tetrahedral bonding angles. The DFT models for both the half and full coverage MMA cases show tetrahedral As bonding. However, the adjacent MMA

move closer together forming a weak Al-Al bond [12]. The calculated DOS for the half and full coverage DMA is shown in Fig. 3(d). As expected the highly strained half coverage case shows a large density of midgap states consistent with the band edge states observed at partial coverage in Fig. 2. The full coverage DMA/InGaAs(001)-(2x4) has a wider bandgap (0.7 vs. 0.5 eV) than the clean surface consistent with passivating the CB edge states on the undercoordinated As atoms. Conversely, the MMA was not as effective as passivating the dangling bond states.

Table 1 shows the binding energies of the adsorbate species. The full coverage cases show higher binding energies, suggesting a driving force to generate a full coverage passivation layer consistent with experimental observation of TMA readily forming a monolayer for adsorbate sites.

DFT-MD calculations were also performed on the unit cell containing a single row As-dimer (Fig. 4a); this As deficient site is observed in more than 50% of the unit cells in STM images [13]. Both half and full coverage DMA on the single dimer unit cell binding energies are shown in Table 1, again showing a driving force to generate a full coverage of DMA. Fig. 4(b) shows the full coverage case on the single As-dimer unit cell. Again the DMA produces tetrahedral bonding for the As surface atoms thereby eliminating their dangling bonds. The DOS, Fig. 4(d), of the full coverage again shows a decrease in the CB edge states. The dissociative chemisorption of TMA to DMA + CH<sub>3</sub> could result in CH<sub>3</sub> chemisorbates. Fig. 4(c) shows a case with two methyl groups bonding to undercoordinated In and Ga row sites; the binding energy of a single methyl group is -2.29 eV relative to CH<sub>3</sub>(g) consistent with activated exothermic desorption to C<sub>2</sub>H<sub>6</sub>(g). The DOS for the coadsorption has a wider bandgap than the clean surface but no improvement over simple passivation by DMA consistent with DMA eliminating As dimers and their dangling bond, making the DMA primarily responsible for surface passivation.

As previously reported, STS and STM experiments show that the TMA passivation of As-rich In<sub>0.53</sub>Ga<sub>0.47</sub>As(001)-(2x4) between 150°C and 280°C produces the same surface structure and electronic characteristics in contrast to TMA passivation of In/Ga-rich In<sub>0.53</sub>Ga<sub>0.47</sub>As(4x2) which only produces a high density adsorbate layer with an electronic structure consistent with unpinning for TMA passivation below 200°C (See Fig. 5)[14]. These results are consistent with the strong binding of TMA to pairs of As dimers on the (2x4) surface as shown in the DFT calculations.

### Capacitance/Conductance Voltage Studies

In order to test if the decreased midgap states due to TMA elimination of As dangling bonds can be observed from a device perspective, capacitance-voltage (CV) and normalized conductance-voltage (GV) analysis were performed on InGaAs samples with and without predosing the surface with TMA prior to 45 cycles of Al<sub>2</sub>O<sub>3</sub>(~3 nm). The ~80 nm As capping layer was desorbed under high

vacuum (1~2x10<sup>-6</sup> Torr). The thickness and doping concentration of the In<sub>0.53</sub>Ga<sub>0.47</sub>As layer were 500 nm and 1.0 x 10<sup>-17</sup>cm<sup>-3</sup>. The a-Al<sub>2</sub>O<sub>3</sub> ALD employed TMA and water vapor with TMA pulsing first in the sequence at substrate temperature of 270°C. 50 nm thick Pd gate electrodes were deposited by thermal evaporation through a shadow mask. Wafer backside contacts of 50 nm Au/20 nm Ti were deposited by e-beam evaporation. Post-metallization FGA was performed at 400°C for 30 min. The ALD system did not have structural analysis tools; however, using the results from the previously described UHV system, low temperature decapping is expected to produce a mostly As-rich (2x4) reconstruction while high temperature decapping should produce a mostly In/Ga-rich (4x2) reconstruction. This is consistent with the better C-V characteristics (Fig. 6) of the low temperature decapped samples without TMA predosing[15].

To test if the effect of TMA predosing on the As-rich surface is temperature dependent, C-V and G-V studies were performed on n-type and p-type low temperature decapped In<sub>0.53</sub>Ga<sub>0.47</sub>As(001) (Fig 7). For both prepulsing temperatures, the inversion characteristics were modestly improved on the n-type samples and greatly improved on the p-type samples. D<sub>it</sub> was extracted from n-type samples by the conductance method at the voltage at which the 1kHz inversion capacitance is maximum. Estimated midgap D<sub>it</sub> values varied: (no predose) = 9.8 x 10<sup>12</sup> cm<sup>-2</sup> eV<sup>-1</sup>; (150°C TMA predose) = 6.9 x 10<sup>12</sup> cm<sup>-2</sup> eV<sup>-1</sup>; (270°C TMA predose) = 6.6 x 10<sup>12</sup> cm<sup>-2</sup> eV<sup>-1</sup>. These results are consistent with the STM/STS results. Note: the dispersion in accumulation is attributed to border traps because it is temperature independent (not shown), which complicates determination of the effect of TMA prepulsing on CB traps states.

To test if the effect of TMA predosing on the In/Ga rich surface is temperature dependent, C-V and G-V studies were performed on n-type and p-type high temperature decapped In<sub>0.53</sub>Ga<sub>0.47</sub>As(001) (Fig 8). For n-type sample prepulsing at lower temperature provided the best inversion characteristics while prepulsing had almost no effect on p-type samples. D<sub>it</sub> was extracted from n-type samples by the conductance method at the voltage at which the 1kHz inversion capacitance is maximum. Midgap D<sub>it</sub> (no predose) = 1.2 x 10<sup>13</sup> cm<sup>-2</sup> eV<sup>-1</sup>; D<sub>it</sub> (150°C TMA predose) = 6.1 x 10<sup>12</sup> cm<sup>-2</sup> eV<sup>-1</sup>; D<sub>it</sub> (270°C TMA predose) = 8.4 x 10<sup>12</sup> cm<sup>-2</sup> eV<sup>-1</sup>. These results also seem consistent with the STM/STS results.

### Conclusion

STM/STS, DFT, and device studies show that even the TMA prepulsing on the As-rich In<sub>0.53</sub>Ga<sub>0.47</sub>As(001)-(2x4) greatly reduces the trap state density consistent with DFT models showing TMA elimination of As-As dimer bonds and passivation of As dangling bond. It is hypothesized that further passivation may require passivation of the metal-metal bonds at In<sub>0.53</sub>Ga<sub>0.47</sub>As(001)-(2x4) defect sites. The author acknowledges funding by the SRC task 1407.008.

## References:

- [1] Y. Hwang, R. Engel-Herbert, S. Stemmer, Applied Physics Letters 98 (2011) 052911.
- [2] A. Molle, L. Lamagna, C. Grazianetti, G. Brammertz, C. Merckling, M. Caymax, S. Spiga, M. Fanciulli, Applied Physics Letters 99 (2011) 193505.
- [3] J.B. Clemens, E.A. Chagarov, M. Holland, R. Droopad, J.A. Shen, A.C. Kummel, Journal of Chemical Physics 133 (2010) 154704.
- [4] J. Shen, D.L. Winn, W. Melitz, J.B. Clemens, A.C. Kummel, ECS Transactions 16 (2008) 463-468.
- [5] W. Melitz, J. Shen, T. Kent, A.C. Kummel, R. Droopad, Journal of Applied Physics 110 (2011) 013713.
- [6] G. Kresse, J. Furthmüller, Computational Materials Science 6 (1996) 15-50.
- [7] G. Kresse, J. Furthmüller, Physical Review B 54 (1996) 11169-11186.
- [8] J.P. Perdew, K. Burke, M. Ernzerhof, Physical Review Letters 77 (1996) 3865-3868.
- [9] J.P. Perdew, K. Burke, M. Ernzerhof, Physical Review Letters 78 (1997) 1396-1396.
- [10] P.E. Blochl, Physical Review B 50 (1994) 17953-17979.
- [11] G. Kresse, D. Joubert, Physical Review B 59 (1999) 1758-1775.
- [12] C. Eckhardt, W. Brezna, O. Bethge, E. Bertagnoli, J. Smoliner, Journal of Applied Physics 105 (2009) 113709-113709-5
- [13] Edmonds et.al ECS Transactions, 50, in press (2012)
- [14] W. Melitz, T. Kent, A.C. Kummel, R. Droopad, I. Thayne, M. Holland, J. Chem. Phys. 136, 154706 (2012)
- [15] [2]Y. Hwang, R. Engel-Herbert, S. Stemmer, Applied Physics Letters 98, 052911 (2011).

	Half Coverage	Full Coverage
Double Dimer		
MMA	-2.20 (eV/MMA)	-2.60 (eV/MMA)
DMA	-2.16 (eV/DMA)	-2.9 (eV/DMA)
Single Dimer		
DMA	-2.79 (eV/DMA)	-3.11 (eV/DMA)

Table 1: DFT calculated binding energies of monomethylaluminum and dimethylaluminum on InGaAs(001)-(2×4) surface for either a unit cell with two (double dimer) or one (single dimer) As-dimers.

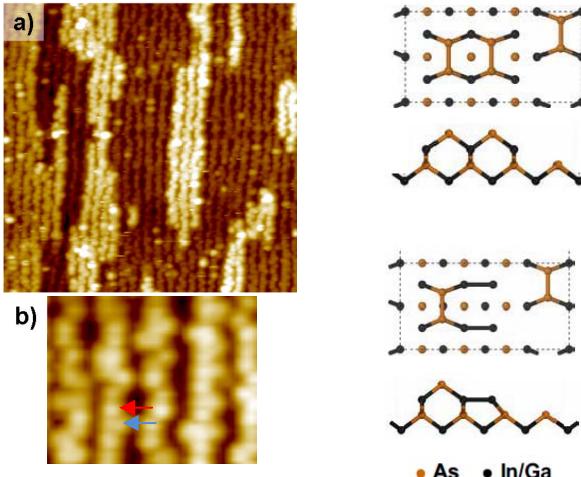


Figure 1: (a) 50x50 nm<sup>2</sup> Filled state STM images of decapped InGaAs(001)-2x4 (b) High resolution STM image showing the zig-zag feature observed on the clean InGaAs(001)-2x4 surface reconstruction which has wide unit cells (blue arrow) and narrow unit cell (red arrow) (c) Model of double As dimer row site; (d) Model of single As dimer row site.

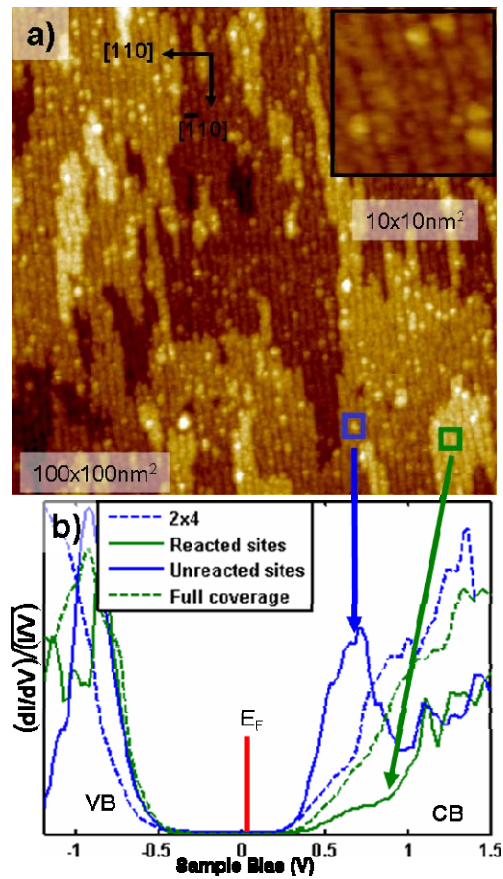


Figure 2: (a) Filled state STM images for 5L TMA doses at 280°C. (b) Point spectroscopy of bright features (unreacted sites) show a LDOS increase at the CB edge. The dashed lines are spectra obtained from the clean 2x4 and full coverage TMA on 2x4 surface.

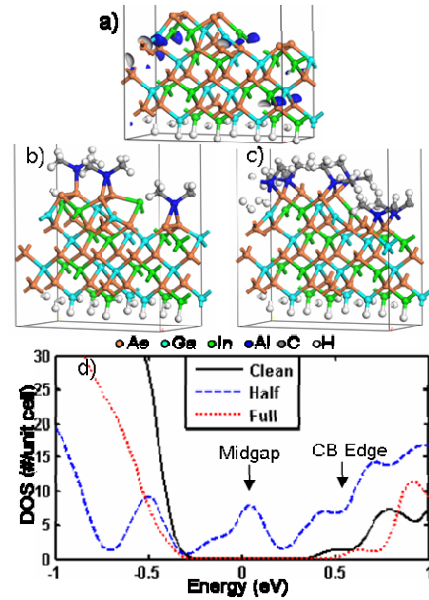


Figure 3: DFT-MD calculations of InGaAs(001)-2x4 (a) clean surface containing a double As-dimer row, (b) half (3 DMA) and (c) full (6 DMA) coverage DMA on double As-dimer unit cell. (d) Calculated DOS. The blue lobes in (a) show the CB edge states from the clean surface.

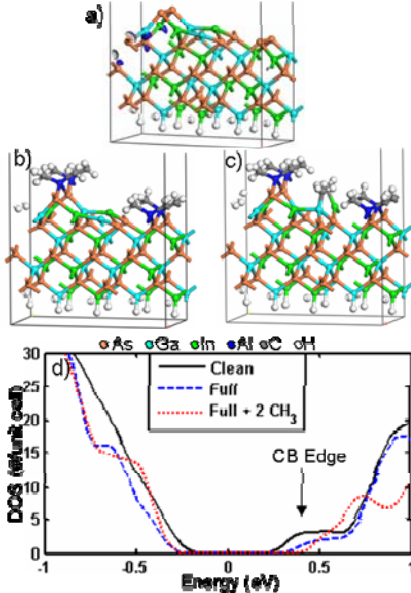


Figure 4: DFT-MD of InGaAs(001)-2x4 with missing As-dimer (a) clean single As-dimer, (b) full (4 DMA) coverage and (c) full coverage with two extra methyl groups bonding to the missing As-dimer site. (d) Calculated DOS

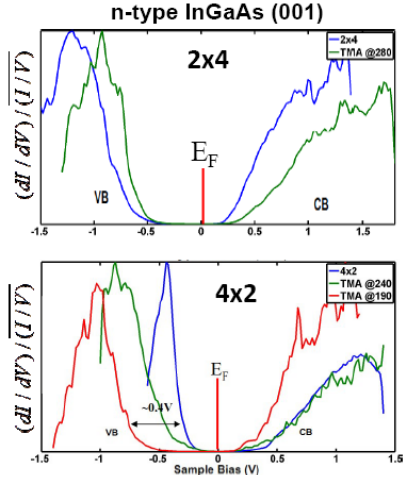


Figure 5: STS of TMA Passivation of n-type In<sub>0.53</sub>Ga<sub>0.47</sub>As(001). Since pinning of In<sub>0.53</sub>Ga<sub>0.47</sub>As(001) moves the Fermi level to the VB, only n-type spectra are shown. (a) TMA passivation of As-rich In<sub>0.53</sub>Ga<sub>0.47</sub>As(001)-(2x4) shows identical STS for all dosing and anneal temperatures between 150°C and 280°C. (b) TMA passivation of In/Ga-rich In<sub>0.53</sub>Ga<sub>0.47</sub>As(001)-(4x2) shows TMA unpins moves the Fermi level ton the CB edge only for TMA dosing below 200°C.

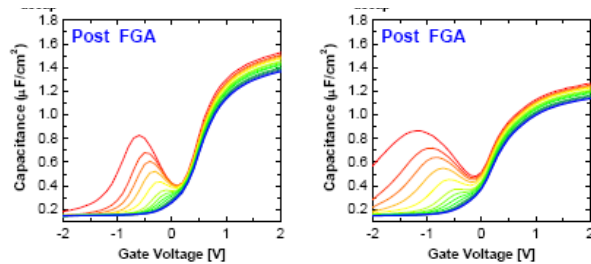


Figure 6 : Effect of As Decapping Temperature on Al<sub>2</sub>O<sub>3</sub>/In<sub>0.53</sub>Ga<sub>0.47</sub>As(001) MOCAPs. As<sub>2</sub> layer were decapped at 370°C (low temperature) or 460°C (high temperature). C-V of low temperature decapped surface(left) shows higher  $C_{acc}$ . than high temperature decapped sample (right). In addition high temperature decapped sample has worse inversion characteristics.

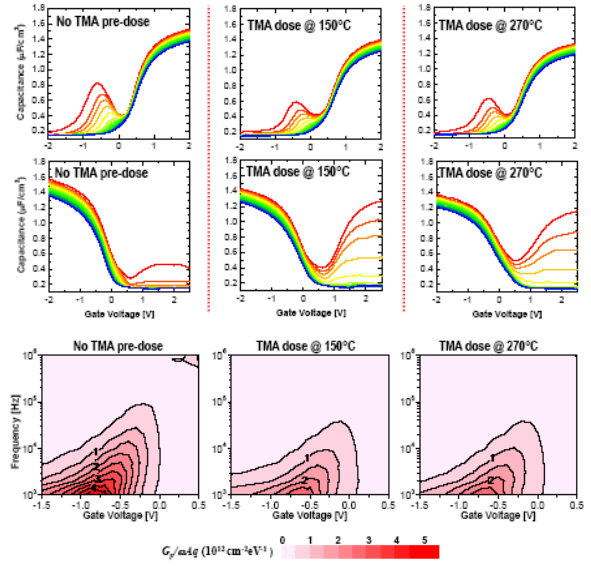


Figure 7: C-V and G-V of TMA prepulsing on Low Temperature Decapped In<sub>0.53</sub>Ga<sub>0.47</sub>As(001) Samples. Prepulsing with TMA was performed at 150°C (middle column) and at 270°C (right column). For both prepulsing temperature the inversion characteristics were modestly improved on the n-type samples and greatly improved on the p-type samples. D<sub>it</sub> was extracted by the conductance method at the voltage at which the 1kHz inversion capacitance is maximum. midgap D<sub>it</sub> (no predose) =  $9.8 \times 10^{12} \text{ cm}^{-2} \text{ eV}^{-1}$ ; D<sub>it</sub> (150°C TMA predose) =  $6.9 \times 10^{12} \text{ cm}^{-2} \text{ eV}^{-1}$ ; D<sub>it</sub> (270°C TMA predose) =  $6.6 \times 10^{12} \text{ cm}^{-2} \text{ eV}^{-1}$ ;

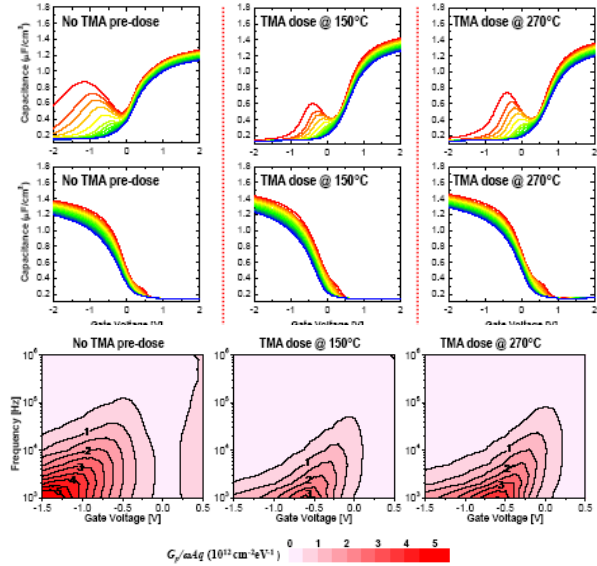


Figure 8: C-V and G-V of TMA prepulsing on High Temperature Decapped In<sub>0.53</sub>Ga<sub>0.47</sub>As(001) Samples. Prepulsing with TMA was performed at 150°C (middle column) and at 270°C (right column). For n-type sample prepulsing at lower temperature provided the best inversion characteristics while prepulsing had almost no effect on -type samples. D<sub>it</sub> was extracted by the conductance method at the voltage at which the 1kHz inversion capacitance is maximum. midgap D<sub>it</sub> (no predose) =  $1.2 \times 10^{13} \text{ cm}^{-2} \text{ eV}^{-1}$ ; D<sub>it</sub> (150°C TMA predose) =  $6.1 \times 10^{12} \text{ cm}^{-2} \text{ eV}^{-1}$ ; D<sub>it</sub> (270°C TMA predose) =  $8.4 \times 10^{12} \text{ cm}^{-2} \text{ eV}^{-1}$ ;